JOURNAL OF GEOPHYSICAL RESEARCH, VOL. 112, D24S44, doi:10.1029/2007JD008830, 2007

Validation of daily erythemal doses from Ozone Monitoring Instrument with ground-based UV measurement data

Aapo Tanskanen,[1] Anders Lindfors,[1] Anu Määttä,[1] Nickolay Krotkov,[2] Jay Herman,[3] Jussi Kaurola,[1] Tapani Koskela,[1] Kaisa Lakkala,[4] Vitali Fioletov,[5] Germar Bernhard,[6] Richard McKenzie,[7] Yutaka Kondo,[8] Michael O'Neill,[9] Harry Slaper,[10] Peter den Outer,[10] Alkiviadis F. Bais,[11] and Johanna Tamminen[1]

Received 16 April 2007; revised 11 July 2007; accepted 14 August 2007; published 21 December 2007.

[1] The Dutch-Finnish Ozone Monitoring Instrument (OMI) on board the NASA EOS Aura spacecraft is a nadir viewing spectrometer that measures solar reflected and backscattered light in a selected range of the ultraviolet and visible spectrum. The instrument has a 2600 km wide viewing swath and it is capable of daily, global contiguous mapping. The Finnish Meteorological Institute and NASA Goddard Space Flight Center have developed a surface ultraviolet irradiance algorithm for OMI that produces noontime surface spectral UV irradiance estimates at four wavelengths, noontime erythemal dose rate (UV index), and the erythemal daily dose. The overpass erythemal daily doses derived from OMI data were compared with the daily doses calculated from the ground-based spectral UV measurements from 18 reference instruments. Two alternative methods for the OMI UV algorithm cloud correction were compared: the plane-parallel cloud model method and the method based on Lambertian equivalent reflectivity. The validation results for the two methods showed some differences, but the results do not imply that one method is categorically superior to the other. For flat, snow-free regions with modest loadings of absorbing aerosols or trace gases, the OMI-derived daily erythemal doses have a median overestimation of 0–10%, and some 60 to 80% of the doses are within ±20% from the ground reference. For sites significantly affected by absorbing aerosols or trace gases one expects, and observes, bigger positive bias up to 50%. For high-latitude sites the satellite-derived doses are occasionally up to 50% too small because of unrealistically small climatological surface albedo.

Citation: Tanskanen, A., et al. (2007), Validation of daily erythemal doses from Ozone Monitoring Instrument with ground-based UV measurement data, *J. Geophys. Res.*, *112*, D24S44, doi:10.1029/2007JD008830.

1. Introduction

[2] Ozone Monitoring Instrument (OMI) is a nadir-viewing spectrometer designed to monitor ozone and other atmospheric species [*Levelt et al.*, 2006]. It is a contribution of the Netherlands's Agency for Aerospace Programs (NIVR) in collaboration with the Finnish Meteorological Institute (FMI) to the NASA Earth Observing System Aura mission. OMI contains two spectrometers that together cover the wavelength range from 270 to 500 nm. The Sun-synchronous polar orbit of the EOS Aura satellite with equator crossing time around 1345 local solar time and the large width of the OMI's viewing swath provide global daily coverage of the sunlit portion of the atmosphere.

[3] OMI continues the Total Ozone Mapping Spectrometer (TOMS) record for total ozone, aerosol, and ultraviolet (UV) measurements. The OMI data are used as an input for a radiative transfer model to estimate the amount of solar UV radiation reaching the Earth's surface. The OMI surface UV algorithm first estimates the clear-sky surface irradiance using the total column ozone measured by OMI, climato-

[1]Finnish Meteorological Institute, Helsinki, Finland.
[2]Goddard Earth Sciences and Technology Center, University of Maryland, Baltimore County, Baltimore, Maryland, USA.
[3]NASA Goddard Space Flight Center, Greenbelt, Maryland, USA.
[4]Arctic Research Centre, Finnish Meteorological Institute, Sodankylä, Finland.
[5]Meteorological Service of Canada/Environment Canada, Downsview, Ontario, Canada.
[6]Biospherical Instruments, San Diego, California, USA.
[7]National Institute of Water and Atmospheric Research, Lauder, Central Otago, New Zealand.
[8]Division of Global Atmospheric Environment, Research Center for Advanced Science and Technology, University of Tokyo, Tokyo, Japan.
[9]Cooperative Institute for Research in Environmental Sciences, University of Colorado, Boulder, Colorado, USA.
[10]Laboratory for Radiation Research, National Institute for Public Health and the Environment (RIVM), Bilthoven, Netherlands.
[11]Laboratory of Atmospheric Physics, Aristotle University of Thessaloniki, Thessaloniki, Greece.

0148-0227/07/2007JD008830$09.00

logical surface albedo, elevation, solar zenith angle, and latitude-dependend climatological ozone and temperature profiles. Next, the clear-sky irradiance is multiplied by a factor that accounts for the attenuation of UV radiation by clouds and nonabsorbing aerosols. This cloud modification factor is derived from the measured reflectance at 360 nm assuming that clouds and aerosols are nonabsorbing at this wavelength. The current algorithm does not account for absorbing aerosols (e.g., organic carbon, smoke, and dust) or trace gases (e.g., NO_2, SO_2), which are known to lead to systematic overestimation of the surface UV irradiance [*Krotkov et al.*, 1998; *Arola et al.*, 2005; *Chubarova*, 2004]. There are, however, plans to implement a correction for absorbing aerosols in the future version of the OMI surface UV algorithm.

[4] Satellite-derived surface UV data based on the TOMS measurements have been extensively validated by comparing them with ground-based measurement data [*Kalliskota et al.*, 2000; *McKenzie et al.*, 2001b; *Chubarova et al.*, 2002; *Fioletov et al.*, 2002; *Cede et al.*, 2004; *Meloni et al.*, 2005; *Arola et al.*, 2005; *Kazantzidis et al.*, 2006]. Most of the validation studies agree that at snow-free conditions, satellite-derived UV data are 0 to 40% higher than ground-based data with the most common biases between 5% and 20%. The smallest biases have been established for unpolluted sites. Past studies with the TOMS data have also revealed systematic underestimation of the surface UV at high-latitude sites when seasonal snow is wrongly interpreted as thick clouds [e.g., *Kalliskota et al.*, 2000; *Krotkov et al.*, 2001, 2002]. Recently, *Kazantzidis et al.* [2006] compared the spectral irradiances (305, 310, and 324 nm) derived from the Earth Probe TOMS data with those measured at four European stations representing different aerosol and cloudiness regimes. They found the largest relative differences between the satellite-derived and measured irradiances at the shortest wavelength, which indicates that the bias was most likely related to tropospheric extinctions not included in the radiative transfer model. *Wuttke et al.* [2003] further emphasized the importance of spectral comparisons in validation of the satellite-derived UV data: spectral validation studies are likely to give hints about the possible sources of the uncertainty.

[5] This study focused on validation of the widely used erythemally weighted data. The satellite-derived erythemal daily doses were compared with those derived from the ground-based measurements of 17 sites and 18 instruments. The main objectives of the study were to gain an initial impression of the applicability of the OMI data for surface UV monitoring and to establish whether the sophisticated plane-parallel-cloud (PPC) model based method for cloud correction [*Krotkov et al.*, 2001] is superior to the simple generalized form of the Lambertian Equivalent Reflectivity (LER) based cloud correction method [*Eck et al.*, 1995; *Krotkov et al.*, 2001]. Additionally, the new surface albedo climatology [*Tanskanen*, 2004] is expected to alleviate the underestimation of the surface UV at high latitudes related to snow/cloud interpretation, and one of the objectives of the validation study was to confirm this.

[6] The OMI surface UV algorithm is presented in section 2, and ground-based spectral UV measurements are described in section 3. Validation method is presented in section 4. In section 5 the validation results are presented and discussed, and their implications are presented in section 6.

2. OMI Surface UV Algorithm and OMUVB Data Product

[7] The OMI surface UV algorithm is an extension of the TOMS UV algorithm developed at NASA Goddard Space Flight Center (GSFC) [*Eck et al.*, 1995; *Krotkov et al.*, 1998; *Herman et al.*, 1999; *Krotkov et al.*, 2001; *Tanskanen et al.*, 2006]. The OMI surface UV algorithm is used for offline production of the global surface UV data using the OMI TOMS total column ozone [*Bhartia and Wellemeyer*, 2002] as input, and this paper is focused on validation of the global surface UV product. The OMI surface UV algorithm is also used in the Very Fast Delivery (VFD) processing system [*Leppelmeier et al.*, 2006]; there the total column ozone input is retrieved with the OMI DOAS total column ozone algorithm [*Veefkind et al.*, 2006]. There is a separate paper about validation of the OMI VFD products [*Hassinen et al.*, 2007].

[8] The OMI surface algorithm estimates the surface UV irradiance by using various lookup tables (LUTs) based on radiative transfer modeling. Estimation of the UV reaching the Earth's surface is divided in two parts. First, the algorithm estimates the surface irradiance assuming clear-sky conditions and uses basic geophysical information to determine solar zenith angle and the distance between the Sun and Earth, total column ozone derived from OMI measurements (OMTO3 product provided by NASA), and climatological surface albedo [*Tanskanen*, 2004]. The surface albedo information required for modeling of the surface UV irradiance is not pointwise surface albedo but rather a regional quantity, referred to as effective albedo, that describes the overall effect of the surface albedo of the surrounding area on the surface UV irradiance. The LUTs for clear-sky irradiance were calculated with the TOMRAD radiative transfer code that uses the auxiliary equations method [*Dave*, 1964]. The radiative transfer model involves a climatological set of latitude-dependent ozone and temperature profiles. *Krotkov et al.* [1998] describe the details of the model and assumptions used in determination of the clear-sky irradiance. They conclude that in the absence of clouds, aerosols, and snow cover, the satellite estimates of the surface UV can have accuracies comparable to the ground-based measurements.

[9] Second, the clear-sky irradiance is adjusted by multiplying it with a cloud modification factor (CMF) that accounts for the attenuation of UV radiation by clouds and nonabsorbing aerosols. We have used two different methods for determination of CMF. The OMI surface UV algorithm determines CMF using a radiative transfer model that assumes plane-parallel cloud (PPC). The LUTs based on the PPC model calculations are used to invert the measured top-of-the-atmosphere radiance into the effective cloud optical depth, τ. The resulting τ is used together with another set of LUTs to determine the spectral attenuation effect on surface UV irradiance relative to the clear sky conditions. The details of the PPC model based cloud correction method are described by *Krotkov et al.* [2001, 2002]. The PPC model does not account for three-dimen-

sional (3-D) effects of clouds. The OMI surface UV data represent the mean surface UV over a wider region (12 × 24 km in nadir) rather than at a point, and therefore the satellite-derived data are not fully comparable with the ground-based measurement data representing local conditions, and more differences between satellite-derived and ground-based data are expected in regions with large variations in topography or surface albedo.

[10] *Krotkov et al.* [2001] presented an alternative cloud correction method: a generalized form of the cloud correction method based on Lambertian Equivalent Reflectivity (LER) [*Eck et al.*, 1995]. LER is determined by solving a simple form of the radiative transfer equation that assumes a pure Rayleigh scattering atmosphere bounded by an isotropically scattering Lambertian surface [e.g., *Bhartia et al.*, 1993], and CMF is obtained from

$$CMF = \frac{1 - LER}{1 - R_s}, \quad (1)$$

where R_s is surface albedo. Because the OMI surface UV overpass data files included the clear-sky erythemal daily dose, LER, and the climatological surface albedo, it was possible to apply the LER based cloud correction method as a postprocessing step. This enabled comparison of the performance of the two alternative cloud correction methods. Estimation of the CMF for mountainous regions is difficult because mountain peaks often rise above the clouds. The current OMI surface UV algorithm applies no cloud correction for altitudes higher than 2.5 km, i.e., clear-sky conditions are assumed for high altitudes.

[11] Absorbing aerosols (e.g., organic carbon, smoke, and dust) or trace gases (e.g., NO_2, SO_2) are known to lead to systematic overestimation of the surface UV irradiance [*Krotkov et al.*, 1998; *Arola et al.*, 2005; *Chubarova*, 2004]. The current OMI surface UV algorithm assumes no aerosols, and therefore the OMI-derived surface UV irradiances are expected to show overestimation for regions that are affected by absorbing aerosols. Greatest overestimations are anticipated for regions affected by urban pollution and for major natural aerosol episodes.

[12] The OMI measurements are nominally made once a day in the afternoon around 1345 local solar time. The exact local overpass time varies by ±50 min and at high latitudes there are often several overpasses per day. However, the UV irradiances are calculated for local solar noon. Corrections are not made for possible changes in cloudiness or total column ozone between the local noon and satellite overpass time. The erythemal daily dose is determined by applying the trapezoidal integration method to the hourly erythemal dose rates calculated assuming the total column ozone and cloud optical depth corresponding to a single OMI measurement.

[13] As the diurnal variation in cloudiness is not taken into account, the daily doses derived from OMI data experience large uncertainty of the order of 20% [*Martin et al.*, 2000]. *Bugliaro et al.* [2006] further investigated the effect of limited temporal sampling of the cloud conditions on the satellite-derived daily surface UV dose and found that already one noon overpass and an averaging over 15 × 15 km is usually sufficient to derive daily doses with maximum uncertainties of about 25–35%. *Martin et al.* [2000] found for the two Alpine sites that they studied, that averaging of the daily doses derived using a single estimate of cloud conditions reduces the effect of diurnal cloud variation and thus, the monthly dose can be accurate within 5%. This finding, however, applies only for sites with no systematic diurnal course cycle of cloudiness. Formation of convective clouds causes increased afternoon cloudiness [e.g., *Meisner and Arkin*, 1987], which may result in underestimated OMI-derived daily dose at some sites because OMI observes the cloud conditions in the early afternoon. The occurrence of convective clouds depends on latitude and climate being common at lowlatitudes and midlatitudes in summer. The effect of the convective clouds on the OMI-derived daily doses was studied by comparing the fore and afternoon doses at each validation site and season and also by estimating the fore and afternoon CMFs derived from the ISCCP-D1 data [*Rossow et al.*, 1996]. Among the validation sites included in this study, the role of the convective clouds was considered to be the most significant for Mauna Loa and Boulder. However, as the OMI surface UV algorithm assumes clear-sky conditions for high altitudes, the OMI-derived doses for Mauna Loa are not affected by convective clouds. In Boulder the bias due to convective clouds shows a clear seasonal pattern: in summer the negative bias exceeds 10%, while the annual average negative bias is only of the order of a few percents. The effect of the convective clouds was found less salient at the other midlatitude sites and insignificant at high-latitude sites included in this study.

[14] A potential cause of systematic positive bias in the OMI-derived daily dose is the occurrence of the morning fog that breaks up by the afternoon. This kind of fog, that has a clear diurnal cycle, can be formed by radiational cooling during the night. However, the radiation fog usually disappears soon after sunrise and has hardly any effect on the accumulated daily dose. Thus we consider radiation fog to have only marginal effect on the OMI-derived daily doses.

[15] The short name for the OMI surface UV data product is OMUVB. The input data for the OMI UV algorithm is Level 2 OMTO3 total column ozone from NASA, while the output is Level 2 OMUVB surface UV irradiance. Both the Level 2 data are in HDF5-EOS format. Each Level 2 OMUVB product file corresponds to a single OMI orbit containing data for some hundred thousand observations over the sunlit portion of one Aura orbit. The primary contents of the OMUVB granules are erythemally weighted daily dose and erythemal dose rate at local solar noon. Additionally, the product includes spectral irradiances at 305.1, 310.1, 324.1, and 380.1 nm also corresponding to the local solar noon. The spectral irradiances assume triangular slit function with full width half maximum of 0.55 nm. The HDF5-EOS files contain also additional information, for example, latitude, longitude, solar zenith angle, and a large number of ancillary parameters that can be used to assess data quality.

[16] The Aura Validation Data Center has produced overpass data by filtering the Level 2 OMUVB data for approximately hundred ground stations where regular surface UV measurements are performed. The overpass data files include all the OMI data whose center of the ground pixel is within 50 km from the measurement site. For high

Table 1. Surface UV Measurement Sites and Instruments Included in the Validation Study

Site	Affiliations	Instruments	Latitude, °N	Longitude, °E	Elevation, m	Characteristics
Jokioinen	FMI	Mk-III 107	60.81	23.50	107	Rural
Sodankylä	FMI	Mk-II 037	67.37	26.63	179	Subarctic
Bilthoven	RIVM	Dilor XY50	52.12	5.20	40	Urban
Thessaloniki	AUTH	Mk-III 086	40.64	22.97	60	Urban
Toronto	MSC	Mk-II 014/015	43.78	−79.47	198	Urban
Churchill	MSC	Mk-II 026	58.74	−94.07	35	Subarctic coast
Saturna Island	MSC	Mk-II 012	48.78	−123.13	178	Pristine
Eureka	MSC	Mk-V 069	80.05	−86.18	315	Arctic coast
Lauder	NIWA	NIWA UVM	−45.04	169.68	370	Pristine
Boulder	NOAA/ESRL	NIWA UV5	39.99	−105.26	1650	semiurban
Mauna Loa	NOAA/ESRL	NIWA UV3	19.53	−155.58	3400	Volcano/Pristine
Tokyo	NIWA/UoT	NIWA UV4	35.65	139.67	20	Megacity
Barrow	NSF	SUV-100	71.32	−156.68	8	Arctic coast
Summit	NSF	SUV-150B	72.58	−38.46	3202	Ice cap
McMurdo	NSF	SUV-100	−77.83	−166.67	183	Antarctic coast
Palmer	NSF	SUV-100	−64.77	−64.05	21	Antarctic coast
Ushuaia	NSF	SUV-100	−54.82	−68.32	3	Pristine

latitudes, OMI provides more than one overpass per day. In this validation study we used the OMI data that were recorded closest to the solar noon (minimum solar zenith angle). Additionally, it was required that the altitude of the satellite pixel center did not differ from the altitude of the measurement site by more than 500 m, which was estimated to cause a maximum uncertainty of the order of ±5% in the OMUVB overpass data [*McKenzie et al.*, 2001a]. The OMUVB data used in this study covered a period from the beginning of the Aura mission to March 2006. The first OMI data correspond to late August 2004, but the instrument started to provide data on a more regular basis in September 2004.

3. Ground-Based Reference Data

[17] The OMI satellite-derived erythemal UV doses were compared with daily doses inferred from the ground-based measurements of spectral UV at 17 measurement sites and 18 instruments. The measurement sites, which are summarized in Table 1, represent different latitudes, elevations, and climatic conditions. More detailed description of local conditions at each validation site is included in the discussion of the validation results. The ground-based instruments include single and double Brewer spectrophotometers, NIWA UV Spectrometer Systems, DILOR XY50 spectrometer, and SUV spectroradiometers. They are within measurement networks maintained by the Finnish Meteorological Institute (FMI), the Netherlands National Institute for Public Health and the Environment (RIVM), Aristotle University of Thessaloniki, Environment Canada, U.S. National Science Foundation (NSF), U.S. National Oceanic and Atmospheric Administration's Earth System Research Laboratory (NOAA ESRL), and New Zealand's National Institute of Water and Atmospheric Research (NIWA). All the instruments are well maintained, calibrated regularly, and their data are corrected for major error sources. Most of the ground-based erythemal daily doses were determined from the measured spectra using the trapezoidal integration method and allowing a maximum gap of 2 h in measurement frequency. The erythemal doses inferred from the ground-based measurement data are considered to be accurate within at least ±10%. The ground-based measurement time series contained occasional gaps in temporal coverage due to various reasons related to instrument calibration and maintenance as well as participation in measurement campaigns. The following subsections provide more detailed information on the instruments deployed within each network.

3.1. European Spectroradiometers

[18] Data from four European measurement sites were included in this study. In Finland, routine spectral UV measurements are performed at two sites. There is a double monochromator Brewer Mk-III spectrophotometer at Jokioinen, whereas at Sodankylä, the surface UV irradiance is measured with a single monochromator Brewer Mk-II. Both Brewers are calibrated with 1000 W lamps traceable to the irradiance scale of Helsinki University of Technology [*Kübarsepp et al.*, 2000]. They are scheduled to perform spectral scans at fixed solar zenith angles, and, additionally, at solar noon each day. This yields a typical scan frequency of once or twice an hour. The data processing includes corrections for dark current, spikes [*Meinander et al.*, 2003], stray light, temperature dependence, and cosine error. Since the single Brewer of Sodankylä provides spectra only up to 325 nm, the measured spectra were extended to longer wavelengths using spectra measured with Bentham spectroradiometers. The method is assessed to result in erythemal dose rates that are accurate within a few percents. Both Finnish instruments have participated actively in international intercomparison campaigns [e.g., *Koskela*, 1994; *Kjeldstad et al.*, 1997; *Bais et al.*, 2001]. In addition, a national comparison is arranged annually. The Sodankylä measurement series has been discussed in detail by *Lakkala et al.* [2003], while for Jokioinen, more detailed information on the measurement procedures is given by *Koskela* [1994]. The Brewer at Jokioinen meets the WMO level S-2 requirements [*Seckmeyer et al.*, 2001] for detection of trends in UV irradiance.

[19] RIVM operates two DILOR XY50 double monochromator spectrometers in Bilthoven, Netherlands. Spectral scans are normally taken every 12 min from sunrise to sunset. The spectrometers are temperature stabilized at 20°C. All spectra are quality flagged and corrected for wavelength scale errors and electronic spikes using the SHICrivm-tool (www.rivm.nl/shicrivm) [*Slaper et al.*, 1995; *Slaper and Koskela*, 1997]. Corrections are applied

for the cosine errors of the input optics and for the effects due to temperature increase of the input optics for high insolation in summer time [*Jäkel et al.*, 2007]. The irradiance calibration is performed using a 1000 W FEL lamp traceable to the primary standard of Physikalisch-Technische Bundesanstalt (PTB). More details are found in the work of *den Outer et al.* [2005]. Spectra produced by RIVM spectrometers agreed within 3–5% with the transportable reference spectroradiometer [*Gröbner et al.*, 2005], and similar results were obtained in recent international spectroradiometer intercomparisons in March 1999, Germany (organized as a part of the EC-project MAUVE), and June 2000, Sweden (NOGIC campaign).

[20] In Thessaloniki, spectral measurements are recorded with a double monochromator Brewer Mk-III spectroradiometer, which is regularly calibrated against NIST traceable standards of spectral irradiance. Spectral measurements are usually performed at steps of 5° solar zenith angle and at local solar noon. The data are corrected for dark current, spikes, temperature dependence and angular response errors. More details on the instrument performance, quality control, corrections and data retrieval can be found in the work of *Bais et al.* [1996, 1998, 2001] and *Garane et al.* [2006]. The daily doses for Thessaloniki were calculated from spectral measurements, which were interpolated to 1 min intervals using collocated measurements with an erythemal detector to account for short-term variations of the radiation field between subsequently measured spectra.

3.2. Canadian Brewer Instruments

[21] The extensive Canadian UV monitoring network deploys both single and double monochromator Brewer spectrophotometers at 12 sites. The stations included in this study are Toronto, Churchill, Saturna Island, and Eureka. Toronto is represented by two Mk-II single monochromator Brewer instruments; the instruments of Churchill and Saturna Island are also Mk-II type, while the instrument in Eureka is a Mk-V single monochromator Brewer (similar to Mk-II for UV measurements). Spectral scans are normally performed from one to four times an hour throughout the day from sunrise to sunset [*McArthur et al.*, 1999]. The Canadian Brewer instruments are calibrated using 1000 W lamps traceable to NIST. The data are corrected for instrument-related systematic errors including cosine error [*Fioletov et al.*, 2002] and the overall uncertainty (2σ) has been estimated at 6% [*Fioletov et al.*, 2001]. This estimate includes a small contribution from not correcting for the temperature dependence of the instruments [*Weatherhead et al.*, 2001]. Field calibrations are normally done in summer and, consequently, data for very hot days and those for the winter months will likely overestimate and underestimate the true values, respectively, by up to 4% [*Fioletov et al.*, 2004]. From the short single monochromator Brewer spectra the erythemal dose rates are calculated using an empirically derived, increased weighting value for the measured 324 nm irradiance. The method introduces an error that is normally less than 2% [*Fioletov et al.*, 2003].

3.3. NIWA Instruments

[22] NIWA UV Spectrometer Systems are deployed at several sites, including stations in collaboration with NOAA ESRL and University of Tokyo. The following stations were included in this study: Lauder (New Zealand), Mauna Loa (Hawaii), Boulder (USA), and Tokyo (Japan). The NIWA UV Spectrometer Systems meet the standards of the Network for the Detection of Atmospheric Composition Change [*McKenzie et al.*, 1997; *Wuttke et al.*, 2006]. The instrument setup has been described by *McKenzie et al.* [1992]. The calibrations for all sites are traceable to the National Institute of Standards and Technology (NIST) via FEL quartz-halogen lamps. Spectral scans are normally taken at 5-degree steps in solar zenith angle and at 10 to 15 min intervals for the period around solar noon. The measurements are corrected for stray light, dark current, nonlinearities in the wavelength drive, temperature dependence of the diffuser [*McKenzie et al.*, 2005], and cosine error. Previous measurement intercomparison campaigns [e.g., *Bais et al.*, 2001] and comparisons with clear sky models [*Badosa et al.*, 2007] give confidence that the absolute irradiances measured by these systems are accurate to within ±5%.

3.4. National Science Foundation's UV Spectral Irradiance Monitoring Network

[23] The UV radiation monitoring network of NSF includes seven mostly high-latitude sites. Five sites were included in this study: McMurdo, Palmer, Ushuaia, Barrow, and Summit. The sites are equipped with SUV-100 spectroradiometers [*Booth et al.*, 1994], with the exception of Summit, where a SUV-150B spectroradiometer [*Wuttke et al.*, 2006] has been deployed. The instruments are designed and manufactured by Biospherical Instruments Inc., which is also responsible for operation of the network and data analysis. The instruments are calibrated with 200 W tungsten-halogen lamps traceable to NIST, and they have successfully participated in several national and international intercomparison campaigns [*Seckmeyer et al.*, 1995; *Lantz et al.*, 2002; *Wuttke et al.*, 2006]. Spectral scans are taken every 15 min. The data used in this study are Version 2 of the NSF network data [*Bernhard et al.*, 2004, 2005, 2006, 2007]. The data have been corrected for the cosine and wavelength errors, and the expanded (2σ) relative uncertainty for erythemal irradiances is approximately 6%.

[24] The NSF Version 2 data includes also additional data products, for example, cloud optical depth and surface albedo. Cloud optical depth is estimated from the reduction of the measured spectral irradiance at 450 nm from a clear-sky model value assuming a thin, homogeneous water cloud (ice cloud for Summit) at approximately 1–3 km above the measurement site. Surface albedo is estimated from the characteristic wavelength-dependent enhancement of global spectral irradiance. These additional data were used for interpretation of the validation results.

4. Validation Method

4.1. Comparison of the Satellite-Derived Doses With Ground-Based Measurements

[25] The satellite-derived erythemal daily doses (EDD_s) were compared with those calculated from the ground-based measurements (EDD_g). The data sets were combined to form a paired daily dose time series. For sites experiencing snow cover, the data pairs were treated separately for high and low surface albedo cases; when the UV surface albedo

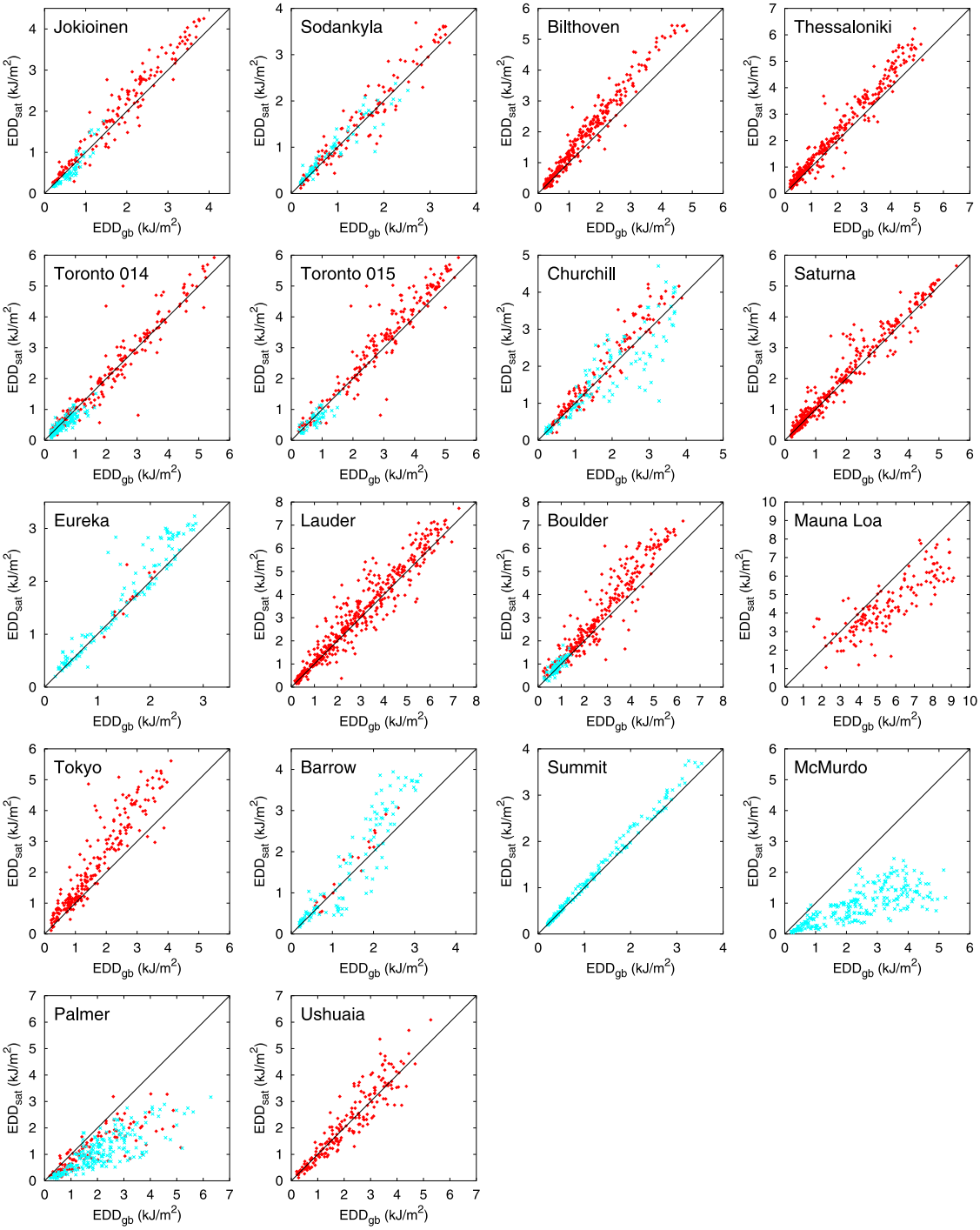

Figure 1. Comparison of the satellite-derived erythemal daily dose with that determined from the ground-based measurements. Red diamonds correspond to days with snow-free conditions, while snow cover cases are marked with blue crosses. Snow information is interpreted from the surface albedo climatology and may diverge from the true snow conditions, and therefore some data pairs may be classified incorrectly.

according to the climatology [*Tanskanen*, 2004] was higher than 0.1 the site was considered to have a snow cover (SC), while the rest of the data were classified as snow-free (SF). Hereafter the terms wintertime and summertime refer to the two separate classes of data pairs for sites where snow cover changes seasonally. It should be noted that because the true snow conditions may diverge from the surface albedo climatology, part of the data pairs were not classified correctly. According to the surface albedo climatology in Summit and McMurdo, the climatological surface albedo was above 0.1 year round. The scattergrams in Figure 1 show comparisons of the erythemal daily doses derived

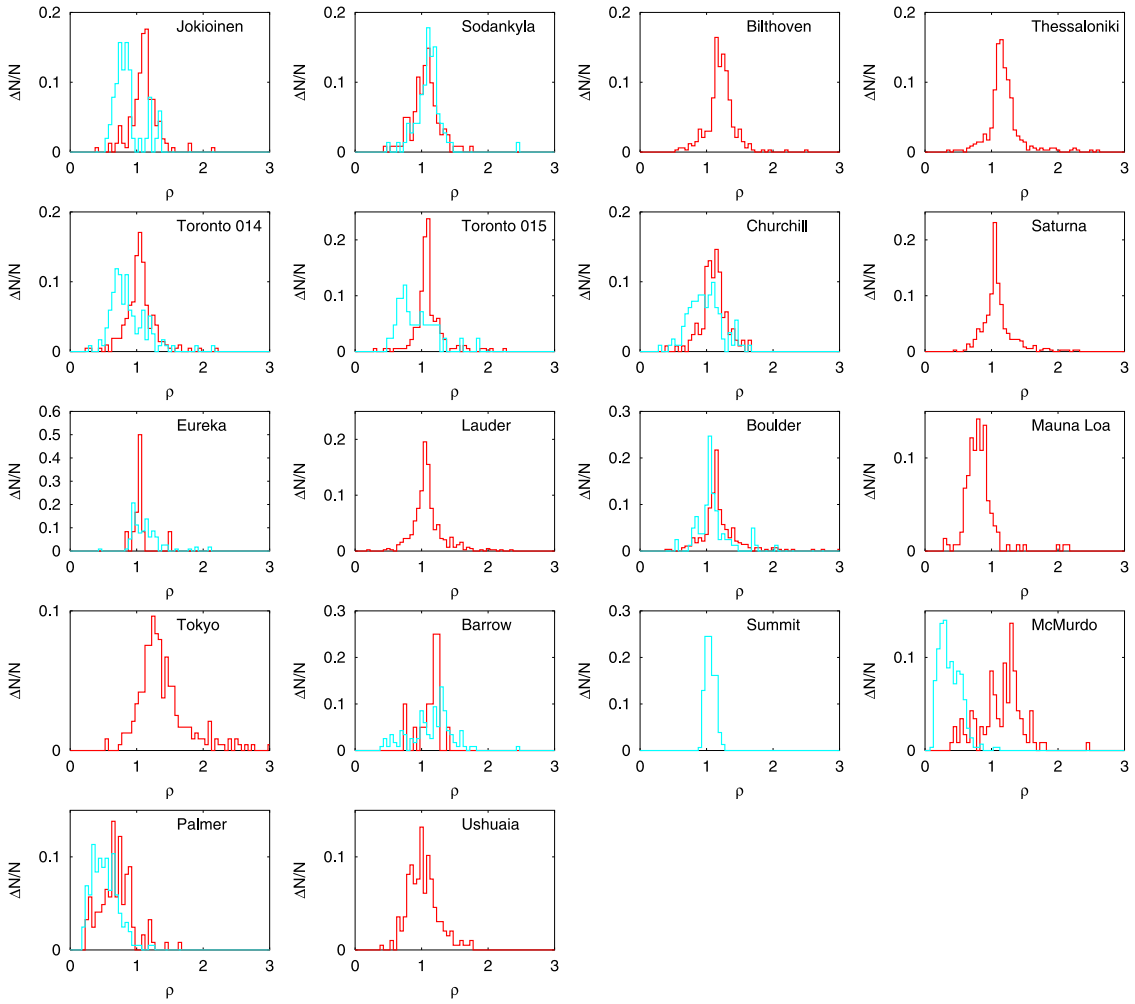

Figure 2. Distributions of the ratio of the satellite-derived erythemal daily dose to those determined from the ground-based measurements. Solid red line corresponds to days with snow-free conditions, while snow cover data is plotted with dashed blue line. Snow information is interpreted from the surface albedo climatology and may diverge from the true snow conditions, and therefore some data pairs may be classified incorrectly.

from OMI data and from ground-based measurements. Red diamonds correspond to days with snow-free conditions, while snow cover cases are marked with blue crosses. The satellite-derived daily doses shown in the scattergrams correspond to the PPC model.

4.2. Validation Statistics

[26] The agreement of the satellite-derived data with the ground-based reference data was assessed by studying the ratio ρ calculated as

$$\rho = \frac{EDD_s}{EDD_g}. \quad (2)$$

The ratio becomes unstable at very low daily doses. Therefore prior to statistical analysis, a threshold filter of 0.2 kJ/m^2 for ground-based daily dose was applied to the time series. The distributions of ρ were plotted for each separate case. The ρ distributions corresponding to the PPC model validation results are shown in Figure 2. Because most of the ρ distributions do not resemble a normal distribution, statistical methods applicable to normal distributions were abandoned. Instead the distributions were analyzed by calculating the median of ρ (denoted as $\tilde{\rho}$), that is less affected by rare abnormal values of ρ. Additionally, we determined the percentage of the satellite-derived data that agrees within ±10, ±20, and ±30% with the reference data, which are denoted as W_{10}, W_{20}, and W_{30}. The validation statistics are shown in Tables 2 and 3 for the PPC and LER validation results, respectively.

5. Results

5.1. General Remarks on the Validation Results

[27] The validation results (Tables 2 and 3) show that at some sites the OMI surface UV algorithm works as intended, but they also reveal the shortcomings of the surface UV algorithm and surface albedo climatology currently in use. The two different cloud correction methods show some systematic features. The PPC model tends to give somewhat higher values of the erythemal daily dose, and for many validation sites the PPC doses differed more

Table 2. Validation Statistics for Comparison of the Daily Erythemal Doses Based on the PPC Model With the Ground-Based Reference Data[a]

Site	Instrument	Surface Conditions[b]	N	$\tilde{\rho}$	W_{10}, %	W_{20}, %	W_{30}, %
Jokioinen	Brewer Mk-III 107	SF	159	1.11	21	67	87
		SC	51	0.82	6	47	71
Sodankylä	Brewer Mk-II 037	SF	121	1.06	45	69	87
		SC	73	1.10	34	67	89
Bilthoven	Dilor XY50	SF	335	1.21	14	44	73
Thessaloniki	Brewer Mk-III 086	SF	348	1.16	24	57	80
Toronto	Brewer Mk-II 014	SF	211	1.05	49	71	86
		SC	118	0.82	18	42	67
Toronto	Brewer Mk-II 015	SF	185	1.08	49	76	88
		SC	42	0.84	24	43	69
Churchill	Brewer Mk-II 026	SF	123	1.13	34	70	84
		SC	111	0.96	31	61	77
Saturna Island	Brewer Mk-II 012	SF	368	1.06	48	73	86
Eureka	Brewer Mk-V 069	SF	12	1.03	83	92	92
		SC	117	1.18	48	72	87
Lauder	NIWA UVM	SF	445	1.06	49	73	85
Boulder	NIWA UV5	SF	281	1.15	22	59	75
		SC	81	1.07	52	72	85
Mauna Loa[c]	NIWA UV3	SF	148	0.80	20	46	70
Tokyo	NIWA UV4	SF	239	1.31	13	27	48
Barrow	SUV-100	SF	20	1.18	20	55	95
		SC	117	1.20	19	32	55
Summit[c]	SUV-150B	PSC	155	1.06	72	99	100
McMurdo	SUV-100	PSC	293	0.35	0	2	2
Palmer	SUV-100	SF	123	0.67	7	23	46
		SC	203	0.51	1	6	15
Ushuaia	SUV-100	SF	197	1.01	35	69	84

[a]N is the number of dose pairs, $\tilde{\rho}$ is the median ratio of the OMI-derived dose to the ground-based dose, and $W_x = P[(100 - x) < 100 \times \rho < (100 + x)]$.

[b]SF = snow-free, SC = snow cover, PSC = permanent snow cover (snow information is interpreted from the surface albedo climatology and may diverge from the true snow conditions, and therefore some data pairs may be classified incorrectly).

[c]No cloud correction because of high elevation.

from the reference data than the doses obtained with the LER method. The results are in accordance with previous findings of *Krotkov et al.* [2001], and *Williams et al.* [2004]. However, it should be remembered that because the current surface UV algorithm does not account for tropospheric extinction, a positive bias is anticipated for sites affected by absorbing aerosols or trace gases. Both cloud correction methods were affected by errors in assumed surface albedo, but the PPC model performed somewhat better in these cases. In the following subsection the validation results are examined site by site starting from simple cases and working towards the more complex cases. The analysis is focused on validation results for the PPC model, but most of the findings are valid also for the LER model.

5.2. Analysis of the Validation Results

[28] The UV measurement installation at Summit is located at the peak of the Greenland ice cap at an elevation of 3202 m a.s.l. The excellent agreement between the satellite-derived doses and the ground-based data for Summit shows that the total column ozone (OMTO3) measured by OMI is accurate, the climatological surface albedo is unbiased, and that the OMI surface UV algorithm produces accurate estimates of the clear sky erythemal daily dose. The algorithm does not apply any cloud correction for sites above 2.5 km. According to the NSF cloud optical depth data for Summit, 95% of the measured cloud optical depths are smaller than 5. The small bias of the satellite-derived doses could be corrected by accounting for the cloud attenuation effect, but it is challenging because current satellite instruments do not provide reliable information on cloud optical depth over snow or ice.

[29] Mauna Loa Observatory (MLO) is located on the northern slope of the Mauna Loa volcano at 3397 m a.s.l. According to the validation results the OMI surface UV algorithm underestimates the erythemal daily dose at MLO. Since the OMI UV algorithm does not apply any cloud correction, the OMUVB data are essentially clear sky surface UV data. The most likely factors causing the observed negative bias are (1) scattering from air and from highly reflecting clouds below the observation site that increase the effective albedo and the observed UV doses, and (2) ozone bias: the satellite-derived ozone column represents an average over a large footprint, whereas the ozone column above the elevated observatory is systematically about 5% less than this mean [*McKenzie et al.*, 2001a]. Figure 3 shows the ratio of the satellite-derived daily dose to ground-based data as a function of the cloud optical depth determined from the OMI measurement data at MLO. The plot illustrates the role of clouds on UV doses at a high elevation measurement site: satellite algorithm performs well at cloud free conditions, but clouds lead to underestimation of the surface UV dose at Mauna Loa.

[30] Saturna Island and Lauder are both pristine midlatitude sites with very low amounts of absorbing aerosols or trace gases. These sites are usually snow-free, and although

Table 3. Validation Statistics for Comparison of the Daily Erythemal Doses Based on the LER Method With the Ground-Based Reference Data[a]

Site	Instrument	Surface Conditions[b]	N	$\tilde{\rho}$	W_{10}, %	W_{20}, %	W_{30}, %
Jokioinen	Brewer Mk-III 107	SF	159	1.05	36	68	81
		SC	51	0.78	10	33	67
Sodankylä	Brewer Mk-II 037	SF	121	1.02	42	64	81
		SC	73	1.09	29	64	92
Bilthoven	Dilor XY50	SF	335	1.10	26	56	79
Thessaloniki	Brewer Mk-III 086	SF	348	1.10	32	61	82
Toronto	Brewer Mk-II 014	SF	211	0.95	44	61	77
		SC	118	0.75	11	22	44
Toronto	Brewer Mk-II 015	SF	185	1.04	46	70	85
		SC	42	0.70	10	24	48
Churchill	Brewer Mk-II 026	SF	123	1.00	29	63	76
		SC	111	0.82	21	43	60
Saturna Island	Brewer Mk-II 012	SF	368	1.03	47	70	82
Eureka	Brewer Mk-V 069	SF	12	1.02	75	92	92
		SC	116	1.09	49	72	84
Lauder	NIWA UVM	SF	445	1.01	45	69	81
Boulder	NIWA UV5	SF	281	1.13	26	60	77
		SC	81	1.07	27	59	79
Mauna Loa[c]	NIWA UV3	SF	148	0.80	20	46	78
Tokyo	NIWA UV4	SF	239	1.22	15	35	59
Barrow	SUV-100	SF	20	1.15	30	65	85
		SC	117	1.20	14	26	42
Summit[c]	SUV-150B	PSC	155	1.06	72	99	100
McMurdo	SUV-100	PSC	292	0.20	0	1	1
Palmer	SUV-100	SF	123	0.51	2	13	23
		SC	201	0.37	0	2	4
Ushuaia	SUV-100	SF	197	0.85	26	48	70

[a]N is the number of dose pairs, $\tilde{\rho}$ is the median ratio of the OMI-derived dose to the ground-based dose, and $W_x = P[(100 - x) < 100 \times \rho < (100 + x)]$.

[b]SF = snow-free, SC = snow cover, PSC = permanent snow cover (snow information is interpreted from the surface albedo climatology and may diverge from the true snow conditions, and therefore some data pairs may be classified incorrectly).

[c]No cloud correction because of high elevation.

there may be snow in the nearby mountains, the effective surface albedo remains low year round. The validation results show that for both Saturna Island and Lauder the systematic overestimation of the satellite-derived erythemal dose is relatively small ($\tilde{\rho}_{PPC} = 1.06$). Furthermore, even a single satellite observation of the cloud conditions provides information for reasonable estimation of the daily dose: nearly half of the satellite-derived daily doses were within 10% from the ground-based reference data. Figure 4 shows the ratio of the satellite-derived daily dose to ground-based data as a function of the OMI cloud optical depth for Lauder. It demonstrates that the error distribution of the satellite-derived UV doses widens with cloud optical depth: cases of heavy clouds are much more challenging for the satellite UV algorithm than cases of mostly clear skies. Therefore better agreement of the satellite-derived doses with ground-based data are anticipated for sites that often experience clear sky conditions in comparison with cloudy sites, and validation results for two climatologically different sites are not directly comparable.

[31] Ushuaia is atmospherically clean monitoring site located in Terra del Fuego at the northern shore of the Beagle Channel. The channel does not freeze, but according to the NSF surface albedo data, snow cover increases the effective albedo up to 0.4 in winter. The satellite-derived daily doses for Ushuaia agree well with the ground-based reference data. The summertime validation results imply that in snow-free conditions the PPC model is superior to the LER method at Ushuaia. Because the ground-based measurement data did not include wintertime data, the wintertime performance of the surface UV algorithm and its albedo climatology at Ushuaia were not established.

[32] The measurement site at Boulder is located at the foot of the Green Mountain near the Boulder city center, and is occasionally affected by urban pollution from nearby Denver. The validation results for Boulder show systematic

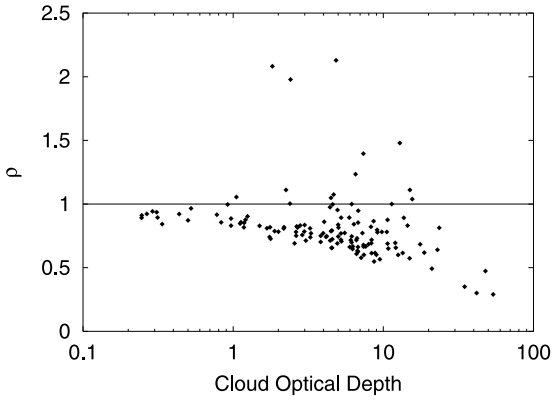

Figure 3. Ratio of the satellite-derived erythemal daily dose to that determined from ground-based measurements as a function of the cloud optical depth determined from OMI data at Mauna Loa Observatory.

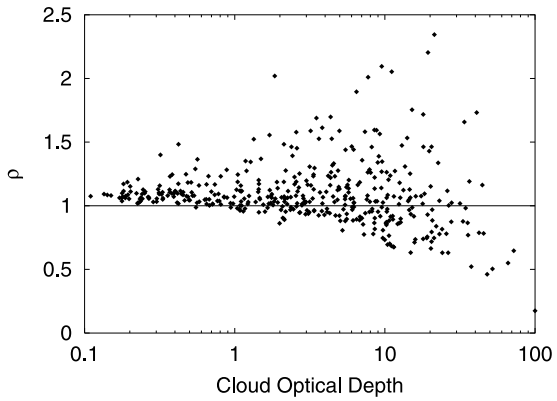

Figure 4. Ratio of the satellite-derived erythemal daily dose to that determined from ground-based measurements as a function of the cloud optical depth determined from OMI data at Lauder.

overestimation of the satellite-derived daily dose both in summer ($\tilde{\rho}_{PPC}$ = 1.15) and winter ($\tilde{\rho}_{PPC}$ = 1.07). Furthermore, as the formation of the convective clouds during the day is considered to cause a negative bias in the OMI-derived daily dose in summer, the observed overestimation is even more significant. According to the Aerosol Robotic Network (AERONET) CIMEL sunphotometer measurements the aerosol loadings at northern midlatitudes are in general larger in summer than in winter [*Holben et al.*, 2001]. Furthermore, as the aerosol single scattering albedo does not show significant seasonal variation [*Delene and Ogren*, 2002], the seasonal variation of the amount of absorbing aerosols is a possible explanation for the seasonally varying bias in the satellite-derived daily dose at Boulder.

[33] Churchill is a small subarctic town located on the west coast of Hudson Bay in a flat and treeless area. In Churchill, snow begins accumulating in November, lasts through April, and is melted by June. The validation results for Churchill show seasonal variation ($\tilde{\rho}_{PPC}$ = 1.13 and 0.96 in summer and winter, respectively). The maximum climatological wintertime surface albedo used by the OMI surface UV algorithm is of the order of 0.7 that is possibly too small for the region and may explain the negative wintertime bias. The summertime positive bias may be caused by aerosols originating from forest fires [*Holben et al.*, 2001; *O'Neill et al.*, 2002]. Forest fires are episodic events and show large variation in their extent, and thus it is difficult to account for their effect on surface UV irradiance.

[34] The observatory of Jokioinen is located in a rural site in the southwestern Finland surrounded by crop fields and mixed boreal forest. The number of snow cover days is typically about 130, and snow cover can increase the effective surface UV albedo up to 0.4. The validation results show overestimation of the surface UV doses in summer ($\tilde{\rho}_{PPC}$ = 1.11) and underestimation of them in winter ($\tilde{\rho}_{PPC}$ = 0.82). The causes of biases are likely similar to those identified for Churchill. However, the possible sources of aerosols and trace gases include urban pollution and smoke from agricultural and forest fires [*Stohl et al.*, 2006].

[35] The measurement site at Toronto is located in the city about 30 km north of Lake Ontario. The average number of snow cover days is 75, and snow cover elevates the effective albedo of the urban area to about 0.35. According to the validation results, the OMI surface UV algorithm overestimates the Toronto summertime daily doses ($\tilde{\rho}_{PPC}$ = 1.05 for Brewer 14, and $\tilde{\rho}_{PPC}$ = 1.08 for Brewer 15). However, the positive bias found for Toronto is smaller than what was established earlier with TOMS UV data [*Fioletov et al.*, 2002]. Formation of convective clouds may partly explain the observed difference in bias. In wintertime the OMI surface UV algorithm underestimates the daily doses ($\tilde{\rho}_{PPC}$ = 0.82 for Brewer 14, and $\tilde{\rho}_{PPC}$ = 0.84 for Brewer 15), suggesting that the surface albedo assumed by the UV algorithm was smaller than the actual effective surface albedo during the validation period.

[36] The measurement site in Barrow is located on the north slope of Alaska at the edge of the Arctic Ocean. The Chukchi Sea is typically covered by ice from November to July, while the flat tundra around the site is usually covered by snow from October to June. According to the NSF surface albedo data the wintertime effective surface UV albedo at Barrow is of the order of 0.8, and decreases down to a few percents as the snow and ice melt. Even though local sources of aerosol and trace gases are small in Alaska, the area is affected by Arctic haze, a circumpolar phenomenon caused by long-range transport of atmospheric pollutants from lower latitudes [*Shaw*, 1995]. Arctic aerosol loadings peak in winter and spring, and as the aerosol mixture includes absorbing components the amount of UV radiation reaching the surface is decreased [*Wetzel et al.*, 2003]. The positive bias of the wintertime validation results for Barrow ($\tilde{\rho}_{PPC}$ = 1.20) could be partly explained by Arctic haze, but it is also possible that the surface albedo is assumed too high. The number of summertime data pairs is too small to make conclusive remarks, which is partly caused by the surface albedo climatology that likely overestimates the surface albedo in late summer.

[37] Eureka is a remote research base on Ellesmere Island and has the lowest average annual temperature and least precipitation of any weather station in Canada. At Eureka snow cover typically starts to accumulate in September and lasts till the end of April. There are no local sources of pollution in Eureka, but the site is affected by Arctic haze [*Ishii et al.*, 1999]. The validation results for Eureka ($\tilde{\rho}_{PPC}$ = 1.03 and 1.18 in summer and winter, respectively) imply elevated positive bias in winter, that could be caused by Arctic haze. It should also be noted that the number of data pairs for snow-free conditions is too small for reliable statistics.

[38] The UV measurement site of FMI's Arctic Research Centre is located 6 km south from the town of Sodankylä. The area is subarctic, and the average number of snow cover days is more than 200. The effective surface albedo ranges from a few percents in summer up to 0.65 in winter [*Arola et al.*, 2003]. There are no major local or effective sources of pollution, but the site is occasionally affected by long-range transport of polluted airmasses [*Aaltonen et al.*, 2006]. According to the validation results, the OMI surface UV algorithm performs well both in summer and winter in spite of the seasonal variation of the surface albedo due to

snow cover. The summertime doses show similar positive bias ($\tilde{\rho}_{PPC}$ = 1.06) to those established for Lauder and Saturna Island. The wintertime doses diverge somewhat more from the reference data ($\tilde{\rho}_{PPC}$ = 1.10), which could be explained either by Arctic haze or by surface albedo climatology.

[39] McMurdo and Palmer are Antarctic coastal sites of NSF's UV Monitoring Network. McMurdo Station is located at Ross Island and surrounded by ice shelves and glaciers. The surface in the immediate vicinity of the instrument is typically covered by snow, but dark volcanic rock may be exposed during summer months (January to March), leading to a drop in effective UV albedo to about 0.75 [*Bernhard et al.*, 2006]. Palmer Station is situated at Anvers Island, west of the Antarctic peninsula. The ocean surrounding the glaciated island is frozen during winter and open during summer, leading to an annual cycle in albedo with values of about 0.8 in winter and 0.4 in summer [*Bernhard et al.*, 2005]. The Antarctic atmosphere is the cleanest globally [*Shaw*, 1982; *Herber et al.*, 1993], and surface UV levels are not significantly affected by aerosols. McMurdo is a dry site and on the average clouds reduce surface UV irradiance by some 10% [*Bernhard et al.*, 2006]. Clouds are more frequent and their optical depths are larger in Palmer, and the average cloud attenuation varies between 28% (October and November) and 42% (February). The validation results show striking underestimation of the satellite-derived surface UV dose at both Antarctic coastal sites included in this study. The modeling error is caused by the climatological surface albedo that deviates substantially from the NSF surface albedo data, which leads to overestimation of cloudiness. According to the satellite-derived cloud modification factors the year-round reduction of the UV doses by clouds is of the order of 60% both for McMurdo and Palmer, that deviates substantially from the observed reductions. The result implies that the surface albedo climatology used by the OMI surface UV algorithm needs to be corrected in order to achieve reasonable satellite-derived UV estimates for Antarctic coastal sites.

[40] RIVM's spectrometer in Bilthoven, Netherlands is located in an urban area. The spectrometer has a free horizon as it is placed on the top of a building. There is only occasionally snow cover in Bilthoven. The validation results show substantial overestimation of the daily erythemal doses by the OMI surface UV algorithm ($\tilde{\rho}_{PPC}$ = 1.21). *Stammes and Henzing* [2000] reported that aerosol optical depth in Bilthoven is typically around 0.4 and has variability of the same order. Furthermore, a comparison of the modeled UV spectra with the measured ones indicates that aerosol optical depth of 0.4 and single scattering albedo of 0.95 are representative values for Bilthoven [*den Outer et al.*, 2005]. Therefore the positive bias of the OMI surface UV estimates is very likely related to aerosols. However, trace gases may also contribute to the bias.

[41] Thessaloniki is an urban coastal site located at the center of the city, about 60 m a.s.l. The surroundings are dominated by concrete buildings from west and east, pine-covered hills to the north, and the sea to the south. Snow cover is very rare and therefore the UV albedo is rather uniform throughout the year, of the order of 0.03. The area is characterized by heavy aerosol load, with particularly absorbing aerosols and increased air pollution [*Bais et al.*, 2005; *Kazadzis et al.*, 2007]. Thus, the degree of overestimation of the Thessaloniki erythemal daily doses by the OMI surface UV algorithm ($\tilde{\rho}_{PPC}$ = 1.16), is reasonable.

[42] The spectrometer in Tokyo is located in the heart of the megacity, one of the most densely populated regions in the world. The measurement horizon in Tokyo is partly obscured by nearby buildings, but their effect on daily doses used in this study is estimated to be less than 2%. The validation results for Tokyo show the largest positive bias ($\tilde{\rho}_{PPC}$ = 1.31). Most of the bias can be attributed to tropospheric extinction by absorbing aerosols and trace gases. Quantification of the effect of the urban pollution on surface UV requires further work. Systematic study of the effect would require comparison of the spectral irradiances that was not included in this study.

5.3. Summary of the Validation Results

[43] Figures 5 and 6 summarize the calculated validation statistics. Figure 5 shows the calculated systematic bias of the OMI-derived erythemal daily doses. Squares indicate that $0.95 < \tilde{\rho} < 1.05$, while triangles denote systematic bias, and the orientation of the triangle shows the sign of the bias. The PPC and LER biases are plotted separately for the snow-free and snow cover cases. In Figure 6 are shown the two key validation statistics ($\tilde{\rho}$ and W_{20}) for all the validation cases. Each point in Figure 6 corresponds to a particular validation case of specific validation site, surface albedo condition, and cloud correction method. The results corresponding to the PPC and LER cloud correction methods show slightly different features, but one method is not categorically superior to the other. However, the advantage of the PPC method of taking into account the spectral dependence of CMF should be kept in mind. Obviously, spectral comparisons are required in order to establish the differences in the spectral irradiances obtained using the two different cloud correction methods.

[44] Three basic subgroups of validation cases can be identified in Figure 6: satisfactory cases, cases with negative bias because of underestimated surface albedo, and cases with positive bias due to tropospheric extinction. Additionally, there are some special cases (Mauna Loa, Summit, Eureka summertime) discussed earlier. It should be noted that the validation cases are not globally representative: high-latitude sites are well represented, but only a few low-latitude or urban sites were included in the study. Nevertheless, the plot gives a rough idea of the expected quality of the OMI-derived daily erythemal doses for a specific site. For flat, snow-free regions with modest loadings of absorbing aerosols or trace gases the OMI-derived daily erythemal doses have a median overestimation of 0–10%, and some 60 to 80% of the doses are within ±20% as compared to the ground reference. For sites significantly affected by absorbing aerosols or trace gases one observes bigger positive bias up to 50%. The high-latitude sites with high surface albedo due to snow cover are particularly challenging for the surface UV algorithm, and for some polar sites the satellite-derived doses are up to 50% too small because of unrealistically small climatological surface albedo that leads to misinterpretation of the observed bright scene as clouds. Thus while the new surface albedo climatology was found reasonable for most of the validation sites, it is faulty for

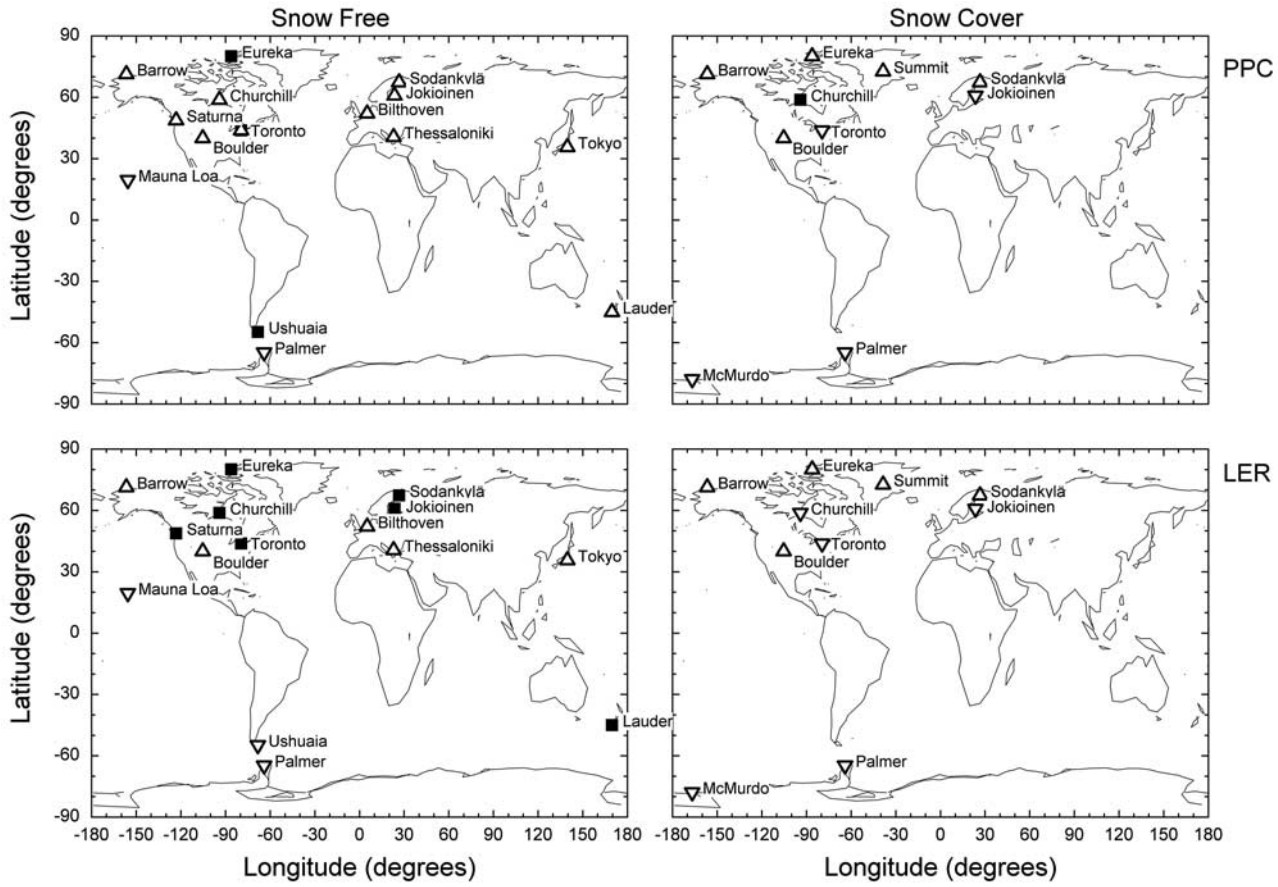

Figure 5. Systematic bias of the OMI-derived erythemal daily doses at the reference sites. Filled squares indicate that $0.95 < \tilde{\rho} < 1.05$, while triangles denote systematic bias: downward pointing triangle refers to negative bias, and upward pointing triangle refers to positive bias.

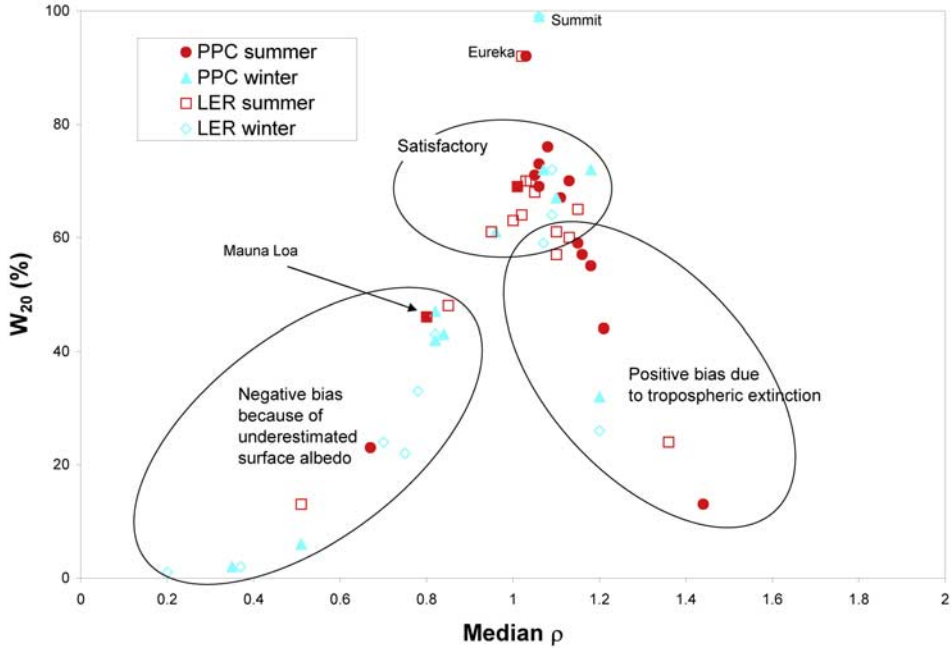

Figure 6. Summary of the key validation statistics. Each point corresponds to a particular validation case of specific validation site, surface albedo condition, and cloud correction method.

Antarctic sites. The validation results imply that there is a need to develop and implement a correction to account for absorbing aerosols and trace gases and to improve the quality of the assumed surface albedo.

6. Conclusions

[45] The daily erythemal surface UV doses derived from the OMI measurements were validated against doses determined from high-quality spectral ground-based measurements. The validation results show that the OMI measurements are suitable for continuation of the global satellite-derived surface UV time series using a surface UV algorithm similar to the original TOMS UV algorithm. Two alternative cloud correction methods were compared: plane-parallel cloud model method and the method based on Lambertian equivalent reflectivity. The validation results do not imply that one cloud correction method is superior to the other. However, a comparison of spectral irradiances would likely show the advantages of the PPC method that accounts for the spectral dependency of cloud modification factor. Furthermore, validation of the spectral irradiances is needed in order to better quantify the positive bias of the satellite-derived UV due to absorbing aerosols and trace gases. Validation results imply that there are two major issues to be solved before the OMI surface UV algorithm can be considered reliable globally: a correction is needed to account for absorbing aerosols and trace gases, and the quality of the assumed surface albedo needs to be improved. The validation tools developed, and the ground-based data gathered for this study lay a solid basis for further development of the OMI surface UV algorithm.

[46] **Acknowledgments.** The Dutch-Finnish built OMI instrument is part of the NASA EOS Aura satellite payload. The OMI project is managed by NIVR and KNMI in the Netherlands. We thank the OMI International Science Team for the satellite data used in this study. The OMI surface UV data were obtained from the NASA Aura Validation Data Center (AVDC). FMI provided Finnish UV measurement data and this work was supported by Finnish Funding Agency for Technology and Innovation (Tekes). RIVM provided spectral UV-measurements and data-analysis for the Bilthoven location and this work was supported by the NIVR as part of the project "OMI and UV-validation" (GO-2005/90) and the EC-project SCOUT. Canadian UV measurement data were provided by MSC/Environment Canada. NIWA provided the UV measurement data of Lauder, Boulder, Mauna Loa, and Tokyo in cooperation with NOAA/ESRL and University of Tokyo. UV measurements and auxiliary data for Barrow, McMurdo, Palmer, Summit, and Ushuaia were provided by the NSF UV Monitoring Network, operated by Biospherical Instruments Inc., with support from the U.S. National Science Foundation's Office of Polar Programs via subcontracts from Raytheon Polar Services Company. This work was performed in the framework of the International ESA/KNMI/NIVR OMI "Announcement of Opportunity for Calibration and Validation of the Ozone Monitoring Instrument," providing early access to provisional OMI data sets and guidance to public OMI data.

References

Aaltonen, V., H. Lihavainen, V.-M. Kerminen, M. Komppula, J. Hatakka, K. Eneroth, M. Kulmala, and Y. Viisanen (2006), Measurements of optical properties of atmospheric aerosols in Northern Finland, *Atmos. Chem. Phys.*, *6*, 1155–1164.

Arola, A., K. Lakkala, A. Bais, J. Kaurola, C. Meleti, and P. Taalas (2003), Factors affecting short- and long-term changes of spectral UV irradiance at two European stations, *J. Geophys. Res.*, *108*(D17), 4549, doi:10.1029/2003JD003447.

Arola, A., S. Kazadzis, N. Krotkov, A. Bais, J. Gröbner, and J. R. Herman (2005), Assessment of TOMS UV bias due to absorbing aerosols, *J. Geophys. Res.*, *110*, D23211, doi:10.1029/2005JD005913.

Badosa, J., R. L. McKenzie, P. V. Johnston, M. Kotkamp, M. O'Neill, and D. J. Anderson (2007), Towards closure between measured and modelled UV under clear skies at four diverse sites, *Atmos. Chem. Phys. Discuss.*, *7*, 1–49.

Bais, A. F., C. S. Zerefos, and C. T. McElroy (1996), Solar UVB measurements with the double- and single- monochromator Brewer ozone spectophotometers, *Geophys. Res. Lett.*, *23*(8), 833–836.

Bais, A. F., S. Kazadzis, D. Balis, C. S. Zerefos, and M. Blumthaler (1998), Correcting global solar ultraviolet spectra recorded by a Brewer spectroradiometer for its angular response error, *Appl. Opt.*, *37*(27), 6339–6344.

Bais, A. F., et al. (2001), SUSPEN intercomparison of ultraviolet spectroradiometers, *J. Geophys. Res.*, *106*(D12), 12,509–12,526.

Bais, A. F., A. Kazantzidis, S. Kazadzis, D. S. Balis, C. S. Zerefos, and C. Meleti (2005), Deriving an effective aerosol single scattering albedo from spectral surface UV irradiance measurements, *Atmos. Environ.*, *39*(6), 1093–1102.

Bernhard, G., C. R. Booth, and J. C. Ehramjian (2004), Version 2 data of the National Science Foundation's Ultraviolet Radiation Monitoring Network: South Pole, *J. Geophys. Res.*, *109*, D21207, doi:10.1029/2004JD004937.

Bernhard, G., C. R. Booth, and J. C. Ehramjian (2005), UV climatology at Palmer Station, Antarctica, in *Ultraviolet Ground- and Space-Based Measurements, Models, and Effects V*, edited by G. Bernhard et al., *Proc. SPIE Int. Soc. Opt. Eng.*, *5886*, 1–12.

Bernhard, G., C. R. Booth, J. C. Ehramjian, and S. E. Nichol (2006), UV climatology at McMurdo Station, Antarctica, based on version 2 data of the National Science Foundation's Ultraviolet Radiation Monitoring Network, *J. Geophys. Res.*, *111*, D11201, doi:10.1029/2005JD005857.

Bernhard, G., C. R. Booth, J. C. Ehramjian, R. Stone, and E. G. Dutton (2007), Ultraviolet and visible radiation at Barrow, Alaska: Climatology and influencing factors on the basis of Version 2 NSF network data, *J. Geophys. Res.*, *112*, D09101, doi:10.1029/2006JD007865.

Bhartia, P. K., and C. W. Wellemeyer (2002), TOMS-V8 total O3 algorithm, in *OMI Algorithm Theoretical Basis Document*, vol II, NASA Goddard Space Flight Cent., Greenbelt, Md. (Available at http://eospso.gsfc.nasa.gov/eos_homepage/for_scientists/atbd/docs/OMI/ATBD-OMI-02.pdf)

Bhartia, P. K., J. Herman, R. D. McPeters, and O. Torres (1993), Effect of Mount Pinatubo aerosols on total ozone measurements from backscatter ultraviolet (BUV) experiments, *J. Geophys. Res.*, *98*(D10), 18,547–18,554.

Booth, C. R., T. B. Lucas, J. H. Morrow, C. S. Weiler, and P. A. Penhale (1994), *The United States National Science Foundation's Polar Network for Monitoring Ultraviolet Radiation*, *Antarctic Res. Ser.*, vol. 62, edited by C. S. Weiler and P. A. Penhale, pp. 17–37, AGU, Washington, D.C.

Bugliaro, L., B. Mayer, R. Meerkötter, and J. Verdebout (2006), Potential and limitations of space-based methods for the retrieval of surface UV-B daily doses: A numerical study, *J. Geophys. Res.*, *111*, D23207, doi:10.1029/2005JD006534.

Cede, A., E. Luccini, L. Nuñez, R. D. Piacentini, M. Blumthaler, and J. Herman (2004), TOMS-derived erythemal irradiance versus measurements at the stations of the Argentine UV Monitoring Network, *J. Geophys. Res.*, *109*, D08109, doi:10.1029/2004JD004519.

Chubarova, N. E. (2004), Influence of aerosol and atmospheric gases on ultraviolet radiation in different optical conditions including smoky mist of 2002, *Dokl. Earth Sci.*, *394*(1), 62–67.

Chubarova, N. E., A. Y. Yurova, N. A. Krotkov, and J. R. Herman (2002), Comparisons between ground measurements of broadband ultraviolet (300 to 380 nm) and total ozone mapping spectrometer ultraviolet estimates at Moscow from 1979 to 2000, *Opt. Eng.*, *41*(12), 2070–3081.

Dave, J. V. (1964), Meaning of successive iteration of the auxiliary equation in the theory of radiative transfer, *Astrophys. J.*, *140*, 1291–1303.

Delene, D. J., and J. A. Ogren (2002), Variability of aerosol optical properties at four North American surface monitoring sites, *J. Atmos. Sci.*, *59*, 1135–1150.

den Outer, P. N., H. Slaper, and R. B. Tax (2005), UV radiation in the Netherlands: Assessing long-term variability and trends in relation to ozone and clouds, *J. Geophys. Res.*, *110*, D02203, doi:10.1029/2004JD004824.

Eck, T. F., P. K. Bhartia, and J. B. Kerr (1995), Satellite estimation of spectral UVB irradiance using TOMS derived ozone and reflectivity, *Geophys. Res. Lett.*, *22*, 611–614.

Fioletov, V. E., L. J. B. McArthur, J. B. Kerr, and D. I. Wardle (2001), Long-term variations of UV-B irradiance over Canada estimated from Brewer observations and derived from ozone and pyranometer measurements, *J. Geophys. Res.*, *106*(D19), 23,009–23,028.

Fioletov, V. E., J. B. Kerr, D. I. Wardle, N. Krotkov, and J. R. Herman (2002), Comparison of Brewer ultraviolet irradiance measurements with total ozone mapping spectrometer satellite retrievals, *Opt. Eng.*, *41*(12), 3051–3061.

Fioletov, V. E., J. B. Kerr, L. J. B. McArthur, D. I. Wardle, and T. W. Mathews (2003), Estimating UV Index Climatology over Canada, *J. Appl. Meteorol.*, *42*(3), 417–433.

Fioletov, V. E., M. G. Kimlin, N. Krotkov, L. J. B. McArthur, J. B. Kerr, D. I. Wardle, J. R. Herman, R. Meltzer, T. W. Mathews, and J. Kaurola (2004), UV index climatology over the United States and Canada from ground-based and satellite estimates, *J. Geophys. Res.*, *109*, D22308, doi:10.1029/2004JD004820.

Garane, K., A. F. Bais, S. Kazadzis, A. Kazantzidis, and C. Meleti (2006), Monitoring of UV spectral irradiance at Thessaloniki (1990–2005): Data re-evaluation and quality control, *Ann. Geophys.*, *24*(12), 3215.

Gröbner, J., et al. (2005), Traveling reference spectroradiometer for routine quality assurance of spectral solar ultraviolet irradiance measurements, *Appl. Opt.*, *44*, 5321–5331.

Hassinen, S., et al. (2007), Description and validation of the OMI very fast delivery products, *J. Geophys. Res.*, doi:10.1029/2007JD008784, in press.

Herber, A., L. W. Thomason, V. F. Radionov, and U. Leiterer (1993), Comparison of trends in the tropospheric and stratospheric aerosol optical depths in the Antarctic, *J. Geophys. Res.*, *98*, 18,441–18,448.

Herman, J. R., N. A. Krotkov, E. Celarier, D. Larko, and G. Labow (1999), Distribution of UV radiation at the Earth's surface from TOMS measured UV-backscattered radiances, *J. Geophys. Res.*, *104*, 12,059–12,076.

Holben, B. N., et al. (2001), An emerging ground-based aerosol climatology: Aerosol optical depth from AERONET, *J. Geophys. Res.*, *106*(D11), 12,067–12,098.

Ishii, S., T. Shibata, T. Nagai, K. Mizutani, T. Itabe, M. Hirota, T. Fujimoto, and O. Uchino (1999), Arctic haze and clouds observed by lidar during four winter seasons of 1993–1997, at Eureka, Canada, *Atmos. Environ.*, *33*(16), 2459–2470.

Jäkel, E., P. N. den Outer, R. Tax, P. C. Göts, and H. A. J. M. Reinen (2007), Improving solar ultraviolet irradiance measurements by applying a temperature correction method for Teflon diffusers, *Appl. Opt.*, *46*, 4222–4227.

Kalliskota, S., J. Kaurola, P. Taalas, J. R. Herman, E. Celarier, and N. Krotkov (2000), Comparison of the daily UV doses estimated from Nimbus7/TOMS measurements and ground-based spectroradiometric data, *J. Geophys. Res.*, *105*, 5059–5067.

Kazadzis, S., et al. (2007), Nine years of UV aerosol optical depth measurements at Thessaloniki, Greece, *Atmos. Chem. Phys. Discuss.*, *7*, 537–567.

Kazantzidis, A., et al. (2006), Comparison of satellite-derived UV irradiances with ground-based measurements at four European stations, *J. Geophys. Res.*, *111*, D13207, doi:10.1029/2005JD006672.

Kjeldstad, B., B. Johnsen, and T. Koskela (Eds.) (1997), The Nordic intercomparison of ultraviolet and total ozone instruments at Izaña, October 1996, *Final Rep. 36*, Finnish Meteorol. Inst., Helsinki.

Koskela, T. (Ed.) (1994), The Nordic intercomparison of ultraviolet and total ozone instruments at Izaña from 24 October to 5 November 1993, *Final Rep. 27*, Finnish Meteorol. Inst., Helsinki.

Krotkov, N. A., P. K. Bhartia, J. R. Herman, V. Fioletov, and J. Kerr (1998), Satellite estimation of spectral surface UV irradiance in the presence of tropospheric aerosols 1: Cloud-free case, *J. Geophys. Res.*, *103*, 8779–8793.

Krotkov, N. A., P. K. Bhartia, J. R. Herman, Z. Ahmad, and V. Fioletov (2001), Satellite estimation of spectral surface UV irradiance: 2. Effect of horizontally homogeneous clouds and snow, *J. Geophys. Res.*, *106*, 11,743–11,759.

Krotkov, N. A., J. R. Herman, P. K. Bhartia, C. Seftor, A. Arola, J. Kaurola, S. Kalliskota, P. Taalas, and I. V. Geogdzhaev (2002), Version 2 total ozone mapping spectrometer ultraviolet algorithm: Problems and enhancements, *Opt. Eng.*, *41*(12), 3028–3039.

Kübarsepp, T., P. Kärhä, F. Manoocheri, S. Nevas, L. Ylianttila, and E. Ikonen (2000), Spectral irradiance measurements of tungsten lamps with filter radiometers in the spectral range 290 nm to 900 nm, *Metrologia*, *37*(4), 305–312.

Lakkala, K., E. Kyrö, and T. Turunen (2003), Spectral UV measurements at Sodankylä during 1990–2001, *J. Geophys. Res.*, *108*(D19), 4621, doi:10.1029/2002JD003300.

Lantz, K., et al. (2002), The 1997 North American interagency intercomparison of ultraviolet spectroradiometers including narrowband filter radiometers, *J. Res. Natl. Inst. Stand. Technol.*, *107*, 19–62.

Leppelmeier, G. W., O. Aulamo, S. Hassinen, A. Mälkki, T. Riihisaari, R. Tajakka, J. Tamminen, and A. Tanskanen (2006), OMI very fast delivery and the Sodankylä satellite data center, *IEEE Trans. Geosci. Remote Sens.*, *44*(5), 1283–1287.

Levelt, P. F., E. Hilsenrath, G. W. Leppelmeier, G. H. J. Van den Oord, P. K. Bhartia, J. Tamminen, J. F. De Haan, and J. P. Veefkind (2006), The Ozone Monitoring Instrument, *IEEE Trans. Geosci. Remote Sens.*, *44*(5), 1093–1101.

Martin, T. J., B. G. Gardiner, and G. Seckmeyer (2000), Uncertainties in satellite-derived estimates of surface UV doses, *J. Geophys. Res.*, *105*(D22), 27,005–27,012.

McArthur, L. J. B., V. E. Fioletov, J. B. Kerr, C. T. McElroy, and D. I. Wardle (1999), Derivation of UV-A irradiance from pyranometer measurements, *J. Geophys. Res.*, *104*, 30,139–30,152.

McKenzie, R. L., P. V. Johnston, M. Kotkamp, A. Bittar, and J. D. Hamlin (1992), Solar ultraviolet spectroradiometry in New Zealand: Instrumentation and sample results from 1990, *Appl. Opt.*, *31*, 6501–6509.

McKenzie, R. L., P. V. Johnston, and G. Seckmeyer (1997), UV spectroradiometry in the network for the detection of stratospheric change (NDSC), in *Solar Ultraviolet Radiation: Modelling, Measurements and Effects*, edited by C. S. Zerefos and A. F. Bais, pp. 279–287, Springer, Berlin.

McKenzie, R. L., P. V. Johnston, D. Smale, B. A. Bodhaine, and S. Madronich (2001a), Altitude effects on UV spectral irradiance deduced from measurements at Lauder, New Zealand, and at Mauna Loa Observatory, Hawaii, *J. Geophys. Res.*, *106*(D19), 22,845–22,860.

McKenzie, R. L., G. Seckmeyer, A. F. Bais, J. B. Kerr, and S. Madronich (2001b), Satellite retrievals of erythemal UV dose compared with ground-based measurements at northern and southern midlatitudes, *J. Geophys. Res.*, *106*, 24,051–24,062.

McKenzie, R. L., J. Badosa, M. Kotkamp, and P. V. Johnston (2005), Effects of the temperature dependence in PTFE diffusers on observed UV irradiances, *Geophys. Res. Lett.*, *32*, L06808, doi:10.1029/2004GL022268.

Meinander, O., W. Josefsson, J. Kaurola, T. Koskela, and K. Lakkala (2003), Spike detection and correction in Brewer spectroradiometer UV spectra, *Opt. Eng.*, *42*, 1812–1819.

Meisner, B. N., and P. A. Arkin (1987), Spatial and annual variations in the diurnal cycle of large-scale tropical convective cloudiness and precipitation, *Mon. Weather Rev.*, *115*, 2009–2032.

Meloni, D., A. di Sarra, J. R. Herman, F. Monteleone, and S. Piacentino (2005), Comparison of ground-based and Total Ozone Mapping Spectrometer erythemal UV doses at the island of Lampedusa in the period 1998–2003: Role of tropospheric aerosols, *J. Geophys. Res.*, *110*, D01202, doi:10.1029/2004JD005283.

O'Neill, N. T., T. F. Eck, B. N. Holben, A. Smirnov, A. Royer, and Z. Li (2002), Optical properties of boreal forest fire smoke derived from Sun photometry, *J. Geophys. Res.*, *107*(D11), 4125, doi:10.1029/2001JD000877.

Rossow, W., A. W. Walker, D. Beuschel, and M. Roiter (1996), International Satellite Cloud Climatology Project (ISCCP) description of new cloud dataset, *WMO/TD 736*, 115 pp., World Clim. Res. Progr., Geneva.

Seckmeyer, G., et al. (1995), Geographical differences in the UV measured by intercompared spectroradiometers, *Geophys. Res. Lett.*, *22*(14), 1889–1892.

Seckmeyer, G., A. Bais, G. Bernhard, M. Blumthaler, C. R. Booth, P. Disterhoft, P. Erikson, R. L. McKenzie, M. Miyauchi, and C. Roy (2001), Instruments to measure solar ultraviolet radiation, part 1: Spectral instruments, *Rep. 125, WMO TD 1066*, World Meteorol. Org., location?.

Shaw, G. E. (1982), Atmospheric turbidity in the polar regions, *J. Appl. Meteorol.*, *21*, 1080–1088.

Shaw, G. E. (1995), The Arctic haze phenomenon, *Bull. Am. Meteorol. Soc.*, *76*, 2403–2412.

Slaper, H., and T. Koskela (1997), Methodology of intercomparing spectral sky measurements, correcting for wavelength shifts, slit function differences and defining a spectral reference, in *The Nordic Intercomparison of Ultraviolet and Total Ozone Instruments at Izana, October 1996*, edited by B. Kjeldstad, B. Johnson, and T. Koskela, pp. 89–108, Finnish Meteorol. Inst., Helsinki.

Slaper, H., H. A. J. M. Reinen, M. Blumthaler, M. Huber, and F. Kuik (1995), Comparing ground-level spectrally resolved UV measurements from various instruments: a technique resolving effects of wavelength shifts and slit widths, *Geophys. Res. Lett.*, *22*(20), 2721–2724.

Stammes, P., and J. S. Henzing (2000), Multispectral aerosol optical thickness at De Bilt, 1997–1999, *J. Aerosol Sci.*, *31*, S283–S284.

Stohl, A., et al. (2006), Arctic smoke – record high air pollution levels in the European Arctic due to agricultural fires in Eastern Europe, *Atmos. Chem. Phys. Discuss.*, *6*, 9655–9722.

Tanskanen, A. (2004), Lambertian surface albedo climatology at 360 nm from TOMS data using moving time-window technique, paper presented at the XX Quadrennial Ozone Symposium, Int. Ozone Comm., Kos, Greece.

Tanskanen, A., N. A. Krotkov, J. R. Herman, and A. Arola (2006), Surface Ultraviolet Irradiance from OMI, *IEEE Trans. Geosci. Remote Sens.*, *44*(5), 1267–1271.

Veefkind, J. P., J. F. de Haan, E. J. Brinksma, M. Kroon, and P. F. Levelt (2006), Total ozone from the Ozone Monitoring Instrument (OMI) using the DOAS technique, *IEEE Trans. Geosci. Remote Sens.*, *44*(5), 1239–1244.

Weatherhead, E., et al. (2001), Temperature dependence of the Brewer ultraviolet data, *J. Geophys. Res.*, *106*(D24), 34,121–34,130.

Wetzel, M. A., G. E. Shaw, J. R. Slusser, R. D. Borys, and C. F. Cahill (2003), Physical, chemical, and ultraviolet radiative characteristics of aerosol in central Alaska, *J. Geophys. Res.*, *108*(D14), 4418, doi:10.1029/2002JD003208.

Williams, J. E., P. N. den Outer, H. Slaper, J. Matthijsen, and G. Kelfkens (2004), Cloud induced reduction of solar UV-radiation: A comparison of ground-based and satellite based approaches, *Geophys. Res. Lett.*, *31*, L03104, doi:10.1029/2003GL018242.

Wuttke, S., J. Verdebout, and G. Seckmeyer (2003), An improved algorithm for satellite-derived UV radiation, *Photochem. Photobiol.*, *77*(1), 52–57.

Wuttke, S., G. Bernhard, J. C. Ehramjian, R. McKenzie, P. Johnston, M. O'Neill, and G. Seckmeyer (2006), New spectrometers complying with the NDSC standards, *J. Oceanic Atmos. Technol.*, *23*(2), 241–251.

A. F. Bais, Laboratory of Atmospheric Physics, Aristotle University of Thessaloniki, GR-54124 Thessaloniki, Greece.

G. Bernhard, Biospherical Instruments, 5340 Riley Street, San Diego, CA 92110-2621, USA.

P. den Outer and H. Slaper, Laboratory for Radiation Research, National Institute for Public Health and the Environment (RIVM), P. O. Box 1, NL-3720 BA Bilthoven, Netherlands.

V. Fioletov, Meteorological Service of Canada/Environment Canada, ARQX 4905, Dufferin Street, Downsview, ON, Canada M3H 5T4.

J. Herman and N. Krotkov, NASA Goddard Space Flight Center, Code 613.3, Greenbelt, MD 20771, USA.

J. Kaurola, T. Koskela, A. Lindfors, A. Määttä, J. Tamminen, and A. Tanskanen, Finnish Meteorological Institute, Erik Palmenin aukio 1, P. O. Box 503, FIN-00101 Helsinki, Finland.

Y. Kondo, Division of Global Atmospheric Environment, Research Center for Advanced Science and Technology, University of Tokyo, 4-6-1 Komaba, Meguro, Tokyo, 153-8904, Japan.

K. Lakkala, Arctic Research Centre, Finnish Meteorological Institute, Tähteläntie 62, FIN-99600 Sodankylä, Finland.

R. McKenzie, National Institute of Water and Atmospheric Research, NIWA Lauder, Private Bag 50 061, Omakau, Central Otago, New Zealand.

M. O'Neill, Cooperative Institute for Research in Environmental Sciences, University of Colorado, 216 UCB, Boulder, CO 80309-0216, USA.